Characterisation of the FBGS Infinityscan®, a code-division multiplexing interrogator for precision and dynamic scanning

63: CHARACTERISATION OF THE FBGS INFINITYSCAN®, A CODE-DIVISION MULTIPLEXING INTERROGATOR FOR PRECISION AND DYNAMIC SCANNING

J. Van Roosbroeck [a*], *E. Lindner* [b], *S. Lochmann* [c], *J. Vlekken* [a*]

[a] FBGS International NV, Geel, Belgium,
[b] FBGS Technologies GmbH, Jena, Germany
[c] Hochschule Wismar, Wismar, Germany

Industrial Sensing, EM009, August 13, 2024, 4:20 PM - 6:10 PM

Abstract – A new fiber optic interrogator has been developed that relies on the principles of Code-Division Multiplexing (CDM), called the 'FBGS InfinityScan®'. It can measure the wavelengths of multiple wavelength-division multiplexed (WDM) sections of Draw Tower Gratings (DTG®s) in series. Wavelength precision measurements and wavelength accuracy estimations for dynamic measurements have been done with this interrogator and will be reported. The precision measurements show that the position of the WDM section in the fiber does not have a significant impact on the measured value. The accuracy estimations for dynamic measurements are compared with a theoretical model and good correspondence has been found. Possible system improvements are proposed to find a suitable compromise between detection accuracy and system speed for large optical sensor networks.

Keywords**:** Code Division Multiplexing, Draw Tower Gratings, InfinityScan**®**, precision, dynamic measurements

1. INTRODUCTION

Fiber Bragg Gratings (FBGs) attract increasing attention as alternative measurement devices [1-3]. Their key advantages are a small form factor, light weight, resistance against electromagnetic interference and the ability to be multiplexed [4]. Typical multiplexing techniques are wavelength-division multiplexing (WDM), optical frequency domain reflectometry (OFDR) or time-division multiplexing (TDM). A promising new multiplexing approach for hundreds or even thousands of serial FBGs is Code-Division Multiplexing (CDM) that uses an autocorrelation method with binary codes to discriminate between sensors with identical wavelengths. Typically, the same WDM section of gratings is repeated multiple times in the same optical fiber. In this way, the combination of CDM with WDM can be used to interrogate large arrays of sensors. Draw Tower Grating® (DTG®) arrays form the ideal sensors to be used in combination with CDM. Dense arrays of DTGs® can be produced in a reliable and cost-effective way [5]. In addition, the reflectivity can easily be tuned to the requested values of around 1% or lower to minimize shadowing. The hybrid CDM-WDM interrogation of thousands of DTG® sensors was already shown in [6]. Other examples of networks containing 4000 (50 × 80), 800 (200 × 4) and 1000 (25 × 40) serial DTGs® with different distances can be found in [7].

In this contribution, the basic principles of CDM are explained. In addition, measurements of the wavelength precision are presented that are done on an exemplary DTG® array that contains multiple WDM sections. Finally, the impact of dynamic changes during sequential reading used by CDM is investigated and experimental results are compared with a theoretical model.

1. PRINCIPLES OF CDM

The CDM setup used in the 'FBGS InfinityScan®' interrogator is depicted in Figure 1. A broadband light source is directly modulated (DM) according to a predetermined binary code. A simple on-off keying is used ('1' is on and '0' is off). Via a circulator, the modulated light enters the sensor array and is reflected by each individual DTG® according to its Bragg wavelength and its location along the fiber. Regular networks are divided into K WDM sections, each containing N DTGs at different wavelengths.

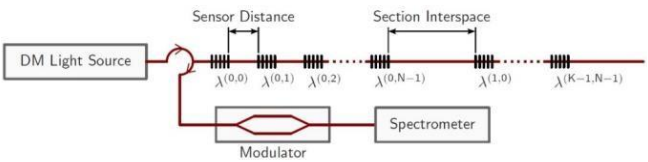

Figure 1: CDM Interrogation System (K: Number of WDM sections, N: Number of sensors per WDM section).

The reflected light is guided via the circulator to a Mach-Zehnder modulator (MZM) that is driven with the same predetermined binary code as the light source but delayed in time. The delay allows the modulation to be synchronized to a specific part of the sensor network depending on the optical path length between light source, DTG® and MZM. At synchronization, every logical '1' of the light source that is reflected at the 'synchronized' section can also pass the modulator and reach the spectrometer. During the integration time period of the spectrometer, all the light of the synchronized code is collected. The spectrum that is measured as such is called the 'direct' spectrum.

However, light from non-synchronized reflections can also coincidentally reach the spectrometer. Due to the specific nature of the code, the probability for this is 50%. Completely removing the influence of non-synchronized sections cannot be achieved with a single code. To remove these contributions, a second spectrum is measured during which the MZM is driven with the inverted version of the predetermined binary code (‘1’↔’0’), holding the same delay as for the direct spectrum. This time, light of the synchronized code is entirely blocked by the MZM due to the inversion (the MZM is closed every time reflected light from the synchronized section arrives). Non-synchronized light however again can pass the modulation stage by coincidence, with a probability of again 50%. It is collected by the spectrometer in the so-called ‘inverted’ spectrum. By taking the difference between the direct and the inverted spectrum, the non-synchronous light is eliminated in the difference spectrum and only the synchronized part remains.

As the synchronization is limited to one specific point within a WDM section, neighbouring sensor peaks will have reduced heights, as a small part of their light is in the inverted spectrum, which is subtracted. This leads to a triangular shaped difference spectrum, the so-called synchronization triangle, see Figure 2. It is the result of a convolution of two rectangular pulses, with its maximum in the synchronization point. The base of the triangle covers one complete WDM section.

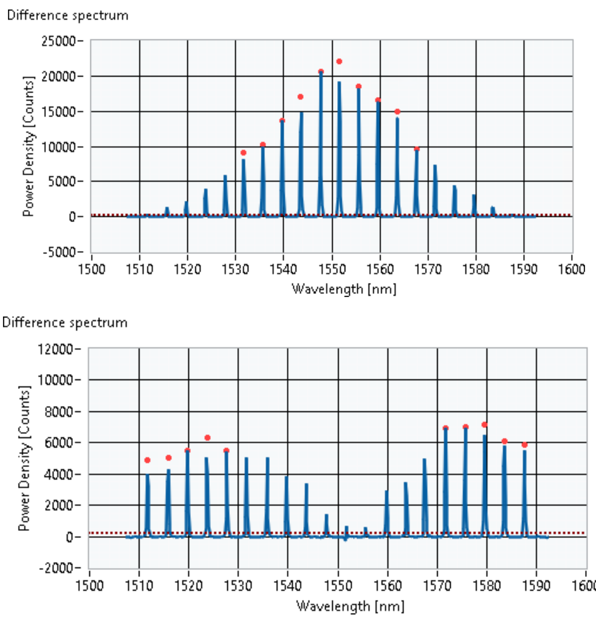

Figure 2: Triangular shaped difference spectra with the delay synchronized to the middle of a particular WDM section (top) and with the delay in between 2 adjacent sections (bottom). Only the higher power peaks are considered for peak tracking, as indicated by the bullets above the peaks.

Due to the triangular shape, the peaks at the sides are suppressed. Therefore, typically 2 delay settings are taken per WDM section: one synchronized to the middle of the section and another in between 2 sections to also measure the peaks at the borders, see also Figure 2. This CDM scheme was already used for the interrogation of 4000 (50 × 80), 800 (200 × 4) and 1000 (25 × 40) serial DTG®s with different network design parameters [6,7].

To illustrate the power of CDM, a sensor from a network containing 4000 DTG®s was strained [8], see Figure 3. The network has 50 identical WDM sections with each section containing 80 different DTG®s. The last sensor from section 50 (sensor 4000) was strained linearly and it shows a wavelength shift that corresponds to the applied strain. The last sensor from the 49th section (sensor 3920) has an identical wavelength, and this stays unaffected since it was not strained. We highlight that the strained sensor’s wavelength overlaps with the Bragg wavelength of other sensors in the network during the shift, which shows no significant impact.

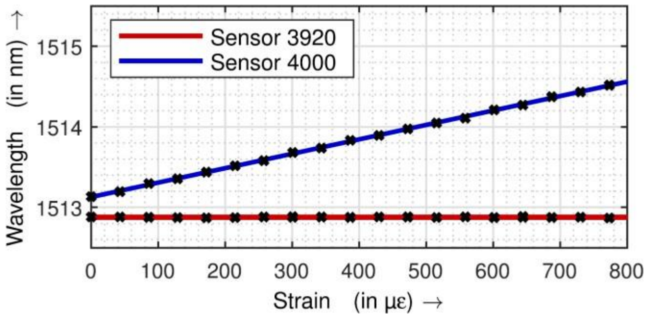

Figure 3: Strain calibration of sensor 4000 (WDM section 50) in a network containing 50 x 80 = 4000 sensors. Sensor 3920 (WDM section 49) has the same wavelength as sensor 4000 and was not strained [8].

2. PRECISION MEASUREMENT IN AN EXEMPLARY CDM SENSING NETWORK

For the precision measurement, a network with 200 DTG®s was interrogated with the ‘FBGS InfinityScan®’. The network contains 10 identical WDM sections, with each 20 DTG®s distributed over the 1510 – 1590 nm bandwidth from low to high wavelengths. The interrogator takes 2 samples per delay setting (for direct and inverted spectrum), and it takes 2 delay settings per WDM section (one in the middle of the section and one at the intersection of 2 adjacent sections). For the first and last section, an additional delay setting needs to be taken. In total, 21 delay settings are chosen, see Figure 4. This is the number of sections multiplied by 2 plus one. The wavelengths from all DTG®s are pieced together from the difference spectra as measured for the 21 different delay settings.

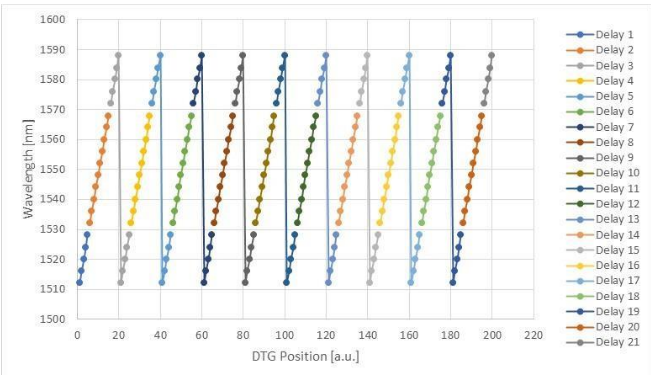

Figure 4: Gratings with their wavelengths ordered as they appear in the fiber. Gratings with the same color are measured together with a specific delay setting.

The interrogator was sampling at 1000 Hz and so every grating in the network is updated at 1000 / (2 x 21) = 23.8 Hz. The wavelengths of all DTG®s were recorded over a period of 20 s, which yields 476 data points per grating. A simple peak detection algorithm was used to calculate the wavelength from the optical spectrum. The algorithm does a Gaussian fit of the 3 highest pixels of each peak. The standard deviation (1σ) with respect to the mean value was calculated for each peak for the complete data set. The results are shown in Figure 5: ordered as a function of the nominal wavelength or ordered as a function of the WDM section index.

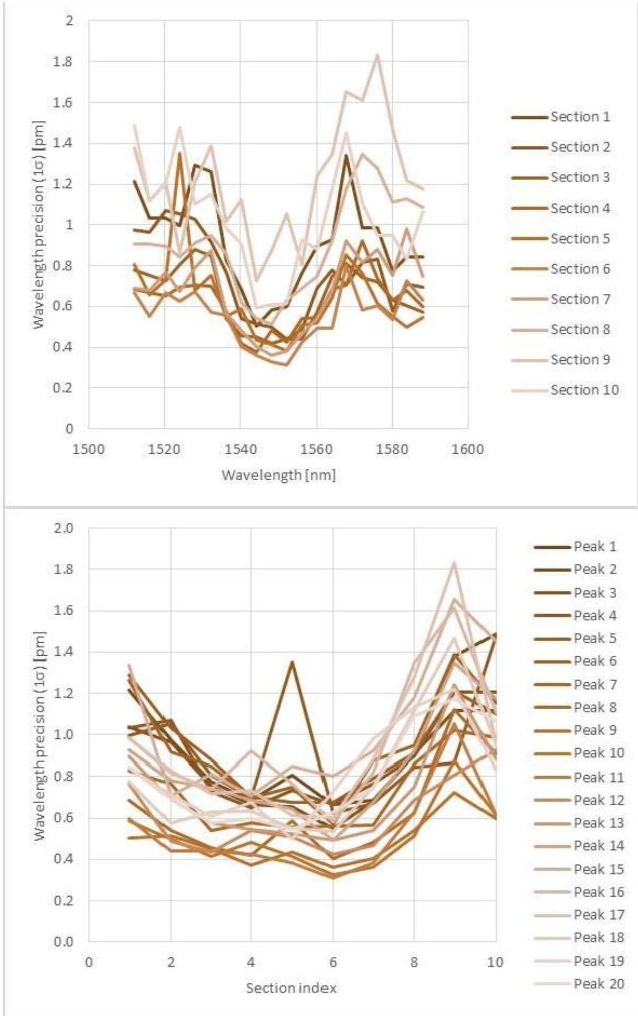

Figure 5: Wavelength precision (1σ) as measured in an exemplary CDM sensing network containing 10 x 20 = 200 DTG®s: ordered as a function of wavelength for each WDM section individually (top) or ordered as a function of the WDM section index for all wavelengths individually (bottom).

The precision is in general in the order of 1 pm. The variation is in the order of ± 0.8 pm. The graph that shows the precision as a function of wavelength indicates the peak power dependence resulting mainly from the Gaussian shaped light source: the larger the peak, the better the precision. Since the peaks from one WDM section are pieced together from 3 separate delay setting measurements, this effect is somehow masked, due to the triangular shape, but it corresponds to what can be expected. This can be understood as follows. Peaks 1-5 and 16 – 20 are measured with a delay setting in between 2 sections. Here, the lowest precision is indeed in general for the lowest and highest wavelengths, which have the highest power because they are closest to the maximum of the triangle. The peaks in the middle (6 – 15) are measured with the delay in the middle of the section. Indeed, the minimum precision for those peaks is found in the middle of the section, where the peaks are closest to the top of the triangle. So, the combination of the used CDM scheme and the shape of the optical source are the dominant parameters for the precision as a function of the wavelength.

A correlation of the precision with the position of the WDM section is less clear or even not existing. An increase in precision was initially expected since the power of the peaks is expected to decrease when advancing further down the fiber because of ‘shadowing’ effects from overlapping FBGs. However, the precision first seems to go down towards the middle of the fiber and then it starts to increase again, which might indicate that the variation of peak powers is not dominated by shadowing effects. This could also experimentally be verified as shown in Figure 6, where the relation between the peak power and precision for peak 11 for the different WDM sections is plotted. As can be seen in the power data, the peak power first increases when advancing further down the fiber and only starts to go down after section 6. It can also be observed that the precision is inversely proportional to the peak power, as expected. These peak power variations can be related to several effects e.g. peak power variations originating from the DTG® inscription process or the delay optimization for each WDM section. They are less affected by shadowing effects for this particular fiber configuration.

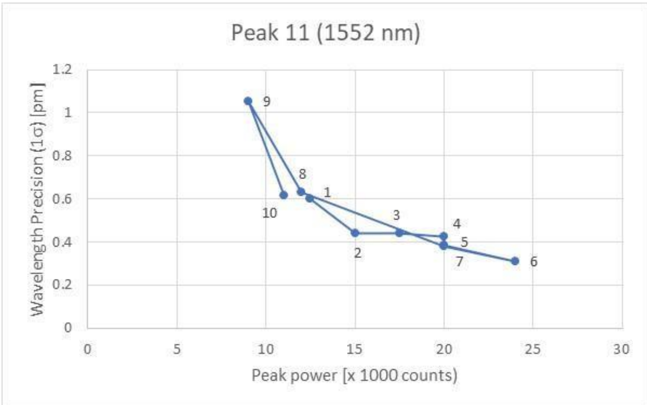

Figure 6: Precision of peak 11 versus its optical peak power for the 10 WDM sections.

3. THEORETICAL CONSIDERATIONS FOR DYNAMIC MEASUREMENTS

The difference spectrum used in CDM is calculated from 2 sequential measurements. In order for this to work properly, it is assumed that the conditions remain static during the time period between both measurements. But when dynamic effects are present, this will in general not be the case.

To investigate the influence of dynamic effects during CDM measurements, simulations were done, see Figure 7. The synchronization triangle shows the percentage of light in the inverted spectrum. To keep the Gaussian shape of the sensor peak, the reflected wavelength of these sensors must not change during the direct and the inverted spectrum acquisition. When the inverted peak is shifted towards positive wavelengths (red dotted line), the peak in the difference spectrum will be deformed, as the subtraction diminishes the right part of the peak in the direct spectrum stronger. Therefore, the maximum of the deformed difference peak leans towards smaller wavelengths. The faster the sensing peak moves during two acquisition steps, the larger the actual wavelength shift between the direct and the inverted peak. Additionally, a slower sampling of an equal speed of wavelength shift leads as well to a larger actual wavelength shift.

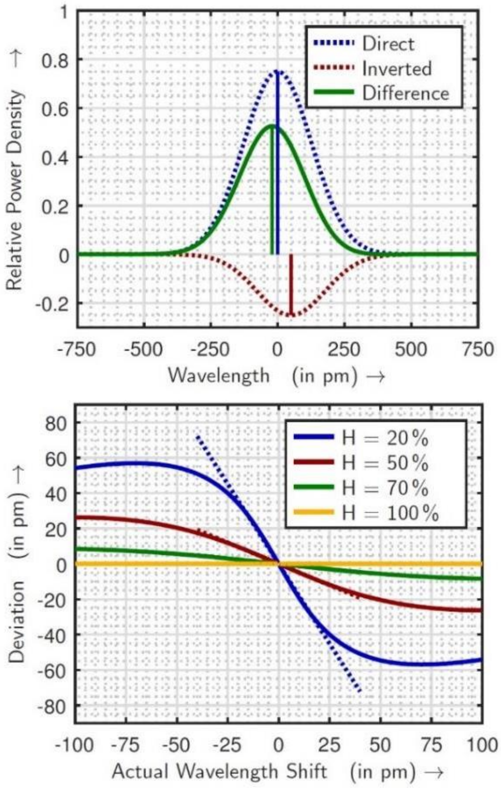

Figure 7: Theoretical approach of dynamic sensor interference: principle of spectral distortion (top) and interference at different heights of the triangle H dependent on the actual wavelength shift (bottom).

In the synchronization point, there is no light in the inverted spectrum, so no deformation of the peak occurs. The greater the distance to this point, the more light is part of the inverted spectrum and thus the larger the deformation and corresponding wavelength deviation will be. This is shown in the bottom graph in Figure 7, which shows the wavelength deviation as a function of the wavelength shift between direct and inverted peak as a function of the triangle heights H. The synchronization point (H = 100 %) serves as a reference, as no deviation occurs. The impact of actual wavelength shifts increases for smaller triangle heights, as the slope of the curves in the origin (dashed lines) indicates. The decreasing deviation for very large actual wavelength shifts can be explained by a vanishing influence of the negative peak, as it shifts outside the area where the direct peak is located.

4. EXPERIMENTAL TRACKING OF DYNAMICALLY STRAINED SENSORS

For the experimental investigation, a (4×40) serial sensor network with 160 DTGs® is used. The sensor distance equals 5 cm, and the section interspace is 80 cm. Dynamic strain is applied to the full length of section 2. The strained section is suspended vertically. Different methods are used to apply a sinusoidal strain profile. The first method uses a weight with a spring attached to the lower end of section 2. Deflecting the spring with the weight leads to large amplitudes but rather low frequency of the applied strain. For the second method, a vibration shaker is attached to the end of section 2. Thus, much higher frequencies can be obtained but with lower amplitudes.

The interrogator is synchronized to the middle of the strained section. Decreasing peak heights due to the synchronization triangle can be found towards smaller and higher wavelengths in the difference spectrum. Thus, the acquisition is identical for all investigated triangle heights in section 2. The acquisition rate is 2 kHz, the difference spectra rate is 1 kHz. Figure 8 shows two measurements where the top graph is the result of the swinging weight: applied strain of 0.5 Hz with an amplitude A of 2.1 nm. The bottom graph is the result of the vibration shaker measurement: applied strain of 40 Hz with an amplitude of 80 pm.

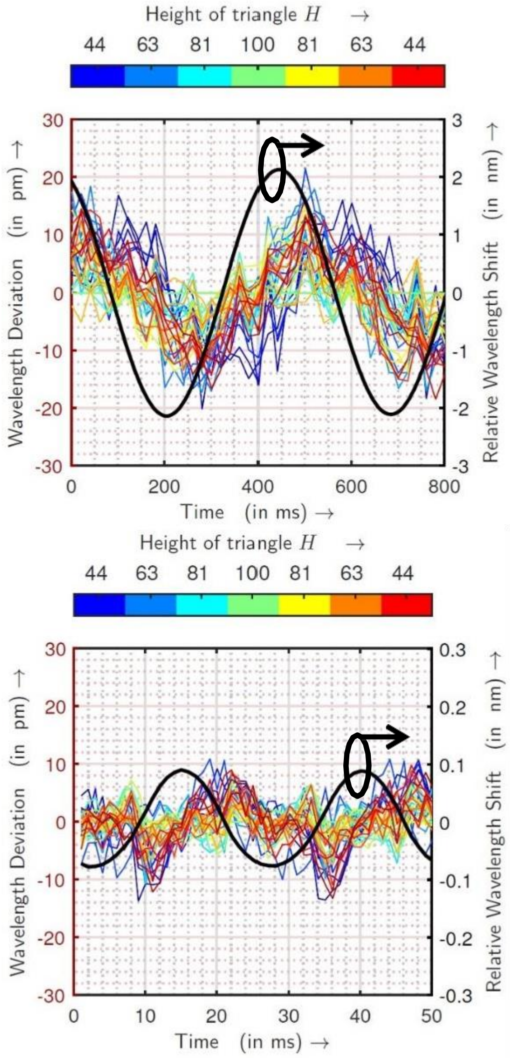

Figure 8: Measured wavelength deviation over time parameterized by the height of the synchronization triangle H in comparison with the reference wavelength shift of the synchronized sensor (H = 100%) at f = 0.5 Hz, A = ± 2.1 nm (top) and f = 40 Hz, A = ± 0.08 nm (bottom).

The obtained difference spectra are analyzed by using a three-point Gaussian fit algorithm to determine the peak wavelengths. To compare the different peaks, first the relative wavelength shift $(\lambda-\lambda_0)/\lambda_0$ is calculated with λ_0 being the mean-value of each tracked peak wavelength. Then the result is multiplied with the Bragg wavelength of the sensor in the synchronization point (H = 100 %). The sensor in the synchronization point serves as a reference for the other sensors and the subtraction leads to the shown deviation results. The triangle heights considered range from 44% to 100%. Lower heights are ignored because they will not occur in practice due to the fact that 3 synchronization points are taken for each WDM section (start, middle and end).

It can be seen that the points with the lowest triangle height (blue and red data points) reach the largest deviation, in good correspondence with the theory. The largest deviations occur where the applied strain changes the fastest, which are the inflection points of the sinusoidal curve. At the extrema, the actual wavelength shift is close to zero, which leads to the minimum of wavelength deviation. It should be noted that other influences, such as data point constellation, accuracy of the peak tracking algorithm and shading effects are also part of the wavelength deviation. The absolute deviation for slow but large sinusoidal applied strain reaches maximum 18 pm for triangle heights down to 44 %. For faster but smaller sinusoidal applied strain, the corresponding absolute deviation reaches up to 13 pm for heights down to 44 %. The corresponding actual wavelength shift between the direct and inverted spectrum can be calculated from the derivative of the curve and results in 32 pm (corresponding to a wavelength rate of 64 nm/s) and 26 pm (corresponding to a wavelength rate of 52 nm/s) for the weight and vibration shaker strain test respectively. Comparing the obtained results with Figure 7, one can see the equivalence with the theoretical approach as it states a deviation of ±15 pm for an actual wavelength shift of ±32 pm and ±12 pm for a shift of ±26 pm at a triangle height of 50 %.

5. CONCLUSIONS

In this work, the InfinityScan® has been presented. It is an interrogator used to measure dense arrays of low reflective DTG®'s. The sensing fibers are typically composed of a repeated pattern of a particular WDM section. The total number of sensors can range from several hundreds to even several thousands. The method to do so is based on Code Division Multiplexing (CDM), in combination with WDM. The operating principles of this method have been presented.

In addition, wavelength precision measurements have been done on an exemplary CDM / WDM sensing network, containing 10 identical WDM sections placed in series within the same optical fiber. Each section contains 20 different DTG®s. The wavelength information is pieced together from the measurement of 21 difference spectra with a specific delay setting. In general, all precision values (1σ) remain within the range of (1.0 ± 0.8) pm and no significant correlation with the position of the WDM section could be observed for the tested fiber configuration.

Finally, also the effect of dynamic measurements has been investigated, both theoretically and experimentally. It could be demonstrated that the sequential read-out during dynamic conditions has a limited influence on the wavelength readings. A stated deviation of ±18 pm could be observed for a wavelength rate of 64 nm/s and ±13 pm for a wavelength rate of ±52 nm/s at a triangle height of 44 %. Results were demonstrated to be in good concordance with the theoretical approach. Therefore, an analytical tool to assess accuracies of different topologies of sensor networks interrogated with the CDM-WDM scheme is established. Further possible improvements could be to have more synchronization points within a section and to use the synchronization triangle only in a narrower part. In addition, increasing the acquisition rate will reduce the wavelength shift between 2 sequential reads and hence a smaller deviation in dynamic measurements can be expected.

REFERENCES

[1] M. A. Riza, Y. I. Go, S. W. Harun, and R. R. J. Maier, **FBG Sensors for Environmental and Biochemical Applications—A Review**, IEEE Sensors Journal 20, 7614–7627, july 2020.

[2] Tochaei, E. N., Fang, Z., Taylor, T., Babanajad, S., and Ansari, F., **Structural monitoring and remaining fatigue life estimation of typical welded crack details in the Manhattan Bridge**, Engineering Structures 231, 111760, March 2021.

[3] Ma, G.-M., Zhou, H.-Y., Li, Y.-B., Zhang, H.-C., Qin, W.-Q., Li, C.-R., and Yan, C., **High-Resolution Temperature Distribution Measurement of GIL Spacer Based on OFDR and Ultraweak FBGs**, IEEE Transactions on Instrumentation and Measurement 69, 3866–3873, June 2020.

[4] Rajan, G., **Optical Fiber Sensors: Advanced Techniques and Applications**, CRC Press, Taylor & Francis Group, Boca Raton, Feb. 2015.

[5] Lindner, E., Mörbitz, J., Chojetzki, C., Becker, M., Brückner, S., Schuster, K., Rothhardt, M., and Bartelt, H., **Draw tower fiber Bragg gratings and their use in sensing technology**, in Fiber Optic Sensors and Applications VIII, Mihailov, S. J., Du, H. H., and Pickrell, G., eds., SPIE, May 2011.

[6] Götten, M., Lochmann, S., Ahrens, A., Lindner, E., and Van Roosbroeck, J., **2000 Serial FBG Sensors Interrogated With a Hybrid CDM-WDM Scheme**, Journal of Lightwave Technology 38, 2493–2503, April 2020.

[7] Götten, M., Lochmann, S., Ahrens, A., Lindner, E., Vlekken, J., and Van Roosbroeck, J., **A CDM-WDM Interrogation Scheme for Massive Serial FBG Sensor Networks**, IEEE Sensors Journal 22, 11290–11296, April 2

[8] M. Götten, S. Lochmann, A. Ahrens, E. Lindner, J. Vlekken, and J. Van Roosbroeck, **4000 Serial FBG Sensors Interrogated with a Hybrid CDM-WDM System**, 2020 IEEE SENSORS, Rotterdam, Netherlands, 2020, pp. 1-4, doi: 10.1109/SENSORS47125.2020.9278764